IEEE Access
Multidisciplinary | Rapid Review | Open Access Journal

Received January 23, 2022, accepted February 11, 2022, date of publication February 16, 2022, date of current version March 2, 2022.

Digital Object Identifier 10.1109/ACCESS.2022.3152191

STBC Identification for Multi-User Uplink SC-FDMA Asynchronous Transmissions Exploiting Iterative Soft Information Feedback of Error Correcting Codes

MOHAMED MAREY[1], (Senior Member, IEEE), AND HALA MOSTAFA[2], (Member, IEEE)
[1]Smart Systems Engineering Laboratory, College of Engineering, Prince Sultan University, Riyadh 11586, Saudi Arabia
[2]Department of Information Technology, College of Computer and Information Sciences, Princess Nourah bint Abdulrahman University, Riyadh 11671, Saudi Arabia

Corresponding author: Mohamed Marey (mfmmarey@psu.edu.sa)

ABSTRACT With the advancement and widespread implementation of multiple-input multiple-output (MIMO) wireless communication systems over the last decade, space-time block coding (STBC) identification has become a critical task for intelligent radios. Previous examinations of STBC identification were focused on single-user transmissions over single-carrier and multi-carrier systems in combination with uncoded broadcasts. Practical systems, on the other hand, contain many users and employ error-correcting codes. For the first time in literature, this work explores the problem of STBC identification for multi-user uplink transmissions in single-carrier frequency division multiple access (SC-FDMA) systems. We take another step closer to real systems by addressing asynchronous transmissions and by conducting multi-user channel estimation. We also exploit the outputs of the channel decoder, which is usually used in many practical systems, to improve the identification and estimation processes. The mathematical analysis demonstrates that the maximum-likelihood (ML) solution of STBC identification, channel estimation, and synchronization can be executed by an iterative approach. The space-alternating generalized expectation-maximization (SAGE) algorithm is used to separate the overlaid signals arriving at the base-station (BS). The parameters under consideration for each user are then updated using an expectation-maximization (EM) processor. Simulation results show that the proposed architecture outperforms other identification methods published in the literature while maintaining a reasonable level of processing time.

INDEX TERMS STBCs identification, SC-FDMA, SAGE, ML estimation.

I. INTRODUCTION

Analysis of wireless signals, aimed at determining the specific transmission parameters of the transmitter used, has been an prominent research area for decades. This analysis is generally referred to as signal identification with military and civilian implications. This has long been used in military applications such as signal interception, radio surveillance, interference detection and mitigation, jamming detection, and electronic warfare [1], [2]. The advent of intelligent radios, reconfigurable transceivers having the ability to alter their transmission settings such as modulation format [3]–[6] and channel coding rate [7]–[11], has heightened interest in signal identification systems in the context of recent civilian applications such as cellular mobile systems and WiFi networks [12], [13].

Signal identification for multiple-input multiple output (MIMO) systems poses unique technical issues that must be taken into account during identifier development. Tracking of signal properties, as well as wireless channel parameters, are challenging in such systems, making it difficult to determine the number and arrangement of transmit antennas. Space-time block coding (STBC) is a MIMO approach in which many copies of a data stream are broadcasted in different time slots via multiple transmit antennas, achieving diversity with a simple receiver structure.

The associate editor coordinating the review of this manuscript and approving it for publication was Yafei Hou.

In single-carrier transmissions contexts, a group of methods relying on the fourth-order moment is suggested to recognize between two STBC signals, Alamouti (AL) and spatial multiplexing (SM) over Nakagami frequency-flat channels in [14]. The authors of [15] investigate the usage of second-order cyclostationarity of two different received signals to classify among several STBC signals. The dispersive characteristics of multipath fading channels is utilized in [16] to discriminate between AL and SM STBC signals. A maximum-likelihood (ML) technique [17] and a Frobenius norm [18] are designed to distinguish between STBC signals. Recently, a convolutional neural network is used to create an STBC classification method [19]. The most significant drawback of [19] is the requirement for a large amount of data in order to accomplish training. In fact, it is not always possible to obtain training data from a source. For example, the categorization of military signals is an excellent illustration of this. Additionally, identifiers are typically implemented on small portable devices with less processing capability. Therefore, if and when it becomes required, retraining will be extremely difficult. This demonstrates the urgent necessity for proposing non-machine learning-based identification methods.

The existing standards' high data rate requirements demand transmissions over wide-band frequency-selective channels. The combination of MIMO systems and multi-carrier (MC) transmissions offers a fascinating solution to the problem of inter-symbol interference, which is a key concern in these conditions. Several wireless communication standards, including WiMAX, LTE, 5G cellular communications, IEEE 802.11n, IEEE 802.11ac, and IEEE 802.11ax, have used MC-MIMO transmissions [20]–[22]. In the framework of MC transmissions, the authors of [23]–[26] use the time-domain correlation functions of two different received signals to classify between AL and SM signals.

Although the earlier studies focused on single-user transmissions, in most real communications systems, the STBC identification process should be carried out in the presence of many users' signals. The main challenge in these multi-user scenarios is that different signals experience different unknown STBC signals, propagation delays, and channel coefficients. Also, the STBC identification process is disrupted by multiple access interference (MAI). As far as the authors' knowledge, this is the first study of its type to focus on the problem of STBC classification in uplink multi-user scenarios for single-carrier frequency division multiple access (SC-FDMA) systems. We provide a novel strategy in which the proposed identifier benefits from the soft information outputs of channel decoders, which are used in a variety of real SC-FDMA systems. The proposed identification algorithm operates also in uplink orthogonal frequency division multiple access (OFDMA) scenarios. Simply one disconnects the FFT and IFFT units from the transmitter and receiving sides, respectively.

The mathematical study in this work reveals that the actual ML solution to STBC identification of multi-user SC-FDMA uplink scenarios is too sophisticated for real applications. Therefore, we resort to a new technique that acts iteratively. The overlaid signals arriving at the base-station (BS) are detached using the space-alternating generalized expectation-maximization (SAGE) algorithm at each iteration [27], [28]. The SAGE algorithm's expectation step uses the soft information of the channel decoders to reduce MAI created by other asynchronous users. This replaces the sophisticated multi-dimensional search with a series of one-dimensional searches. The resulting design is evocative of parallel STBC identification for multiple users, in which MAI is re-constructed and eliminated from the received signal to optimize each user's identification process. Channel estimation and timing synchronization algorithms are also designed to complement the proposed identification technique. Notably, the feedback provided by an uncoded data detector has been used to solve several difficulties that have arisen in multi-carrier systems, such as equalization [29], [30] and frequency synchronization [27], [28]. However, this is the first time it has been used in conjunction with coded transmissions in STBC identification for such systems.

The remainder of the study is broken down into the following sections. The problem statement and system structure are discussed in Section II. The proposed identification algorithm is described in Section III. Practical considerations and interpretations are reported in Section IV. Simulation results are discussed in Section V. Concluding remarks are presented in Section VI.

II. SIGNAL MODEL AND PROBLEM FORMULATION

We consider a wireless uplink multi-user SC-FDMA system with K active users as shown in figure 1. The total number of subcarriers $\mathcal{M}$ is splitted into $U \geq K$ subgroups. Each subgroup has $M_s = \mathcal{M}/U$ subcarriers which are uniquely allocated to an active user, not to other users in the same time slot. Mathematically speaking, the set of subcarriers reserved to user k, $S^{(k)}$, satisfies $\bigcup_{k=0}^{K-1} S^{(k)} = \{0, 1, \cdots, \mathcal{M}-1\}$ and $S^{(k)} \bigcap S^{(k')} = \phi$ for $k \neq k'$. Here ϕ refers to the null set. Each user k has $P^{(k)}$ transmit antenna elements.

A. TRANSMITTER

A sequence of binary information digits of user k passes through a channel encoder of rate $c^{(k)}$ which adds redundancy bits to correct errors produced in the transmission. The coded bits are interleaved and then mapped to complex data symbols which are delivered from a certain set of components $\Phi^{(k)}$ of unit energy. Here, we do not impose any constraints on modulation, coding, and interleaving parameters of each user. A few pilots are encapsulated into data symbols to initialize the identification process as shown later on. The resulting sequence is split into $Z^{(k)}$ vectors, each has M_s symbols. Let $\mathbf{a}_z^{(k)} = \left[a_z^{(k)}(0), \cdots, a_z^{(k)}(M_s-1)\right]$ be the zth vector, with $a_z^{(k)}(m)$ being its mth element.

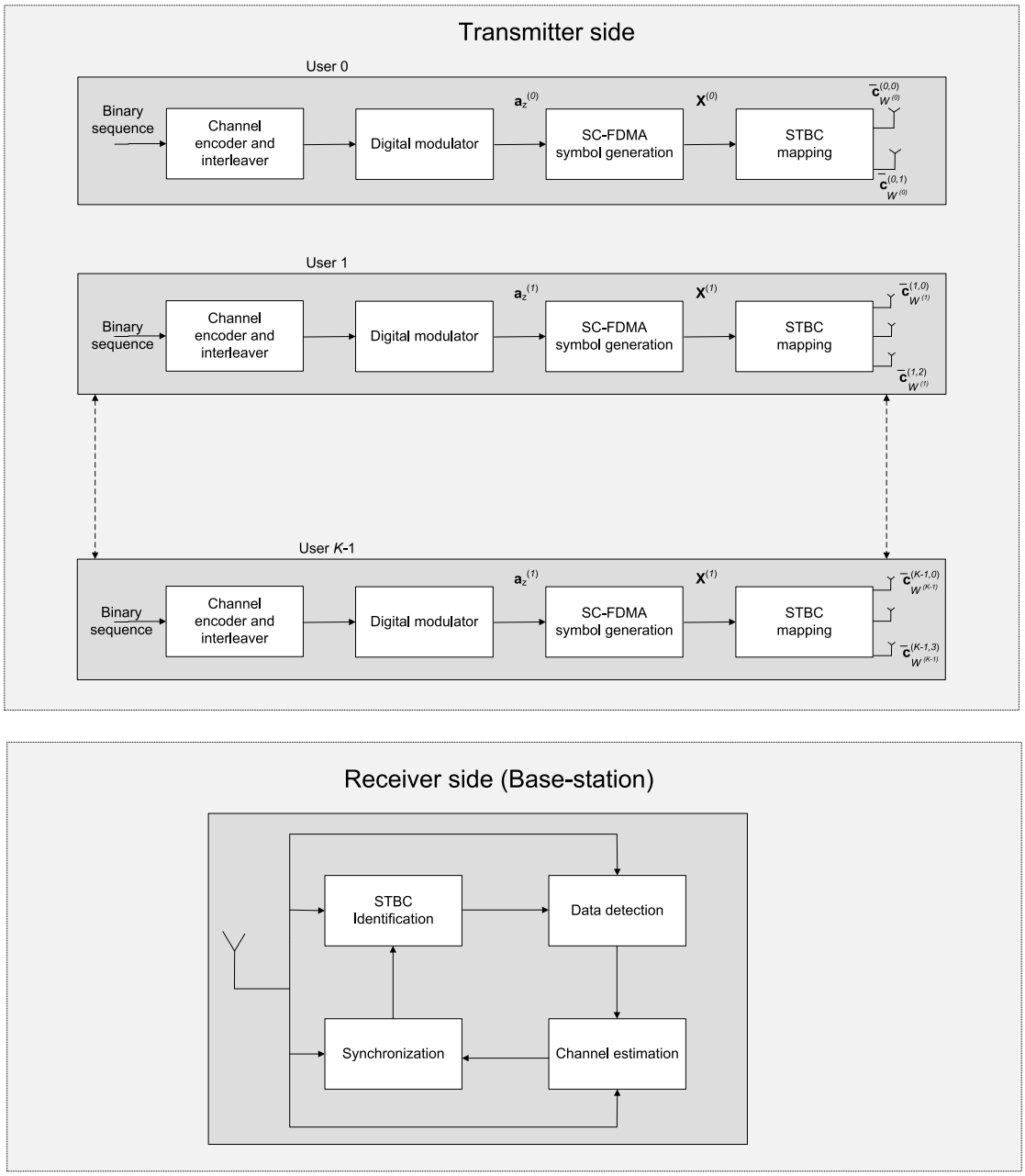

FIGURE 1. Conceptual block diagram of a SC-FDMA system.

After the M_s-point fast Fourier transform (FFT) operation, the corresponding frequency-domain samples $\mathbf{d}_z^{(k)} = \left[d_z^{(k)}(0), \cdots, d_z^{(k)}(M_s-1)\right]$ are expressed as

$$d_z^{(k)}(l) = \frac{1}{\sqrt{M_s}} \sum_{m=0}^{M_s-1} a_z^{(k)}(m) \exp\left(-j2\pi ml/M_s\right), \quad (1)$$

where $d_z^{(k)}(l)$ is the lth sample of $\mathbf{d}_z^{(k)}$ and $j = \sqrt{-1}$. The elements of $\mathbf{d}_z^{(k)}$ modulate M_s subcarriers according to interleaved mapping defined as

$$\tilde{d}_z^{(k)}(m) = \begin{cases} d_z^{(k)}(l) & m = k + lU \\ 0 & \text{otherwise,} \end{cases} \quad (2)$$

and localized mapping characterized as

$$\tilde{d}_z^{(k)}(m) = \begin{cases} d_z^{(k)}(l) & m = kM_s + l \\ 0 & \text{otherwise,} \end{cases} \quad (3)$$

where $0 \le k \le K-1$ and $0 \le l, m \le M_s - 1$. The transformation of $\left[\tilde{d}_z^{(k)}(0), \cdots, \tilde{d}_z^{(k)}(\mathcal{M}-1)\right]$ into an SC-FDMA symbol is conducted by using an $\mathcal{M}-$point

inverse FFT (IFFT) with including a cyclic prefix of length ν. We write the m_1th sample of zth SC-FDMA symbol $\mathbf{x}_z^{(k)} = \left[x_z^{(k)}(-\nu), \cdots, x_z^{(k)}(\mathcal{M}-1)\right]$ of user k as

$$x_z^{(k)}(m_1) = \frac{1}{\sqrt{\mathcal{M}}} \sum_{m_1=0}^{\mathcal{M}-1} \tilde{d}_z^{(k)}(m_2) \exp\left(j2\pi m_1 m_2/\mathcal{M}\right), \quad (4)$$

where $m_1 = -\nu, \cdots, \mathcal{M}-1$. SC-FDMA symbols of user k, $\bar{\mathbf{x}}^{(k)} = \left[\mathbf{x}_0^{(k)}, \cdots, \mathbf{x}_{Z^{(k)}-1}^{(k)}\right]$, are fed to a space-time encoder which transmits each $Z_1^{(k)}$ SC-FDMA symbols through $P^{(k)}$ antennas in $Z_2^{(k)}$ time slots. For example, the STBC $\left(Z_1^{(k)}=2,\, Z_2^{(k)}=2,\, P^{(k)}=2\right)$ called Alamouti code [31] conveys a block of two SC-FDMA symbols $\left[\mathbf{x}_z^{(k)}, \mathbf{x}_{z+1}^{(k)}\right]$ through two antenna components in two continuous periods of time. In the first period, $\mathbf{x}_z^{(k)}$ and $\mathbf{x}_{z+1}^{(k)}$ are broadcasted from the first and second antenna components, respectively. In the subsequent period, $-\mathbf{x}_{z+1}^{(k)*}$ and $\mathbf{x}_z^{(k)*}$ SC-FDMA symbols are sent from the first and second antenna components, respectively. Here, $*$ refers to conjugate operation.

Each user k selects a STBC scheme, denoted as $\varpi^{(k)}$, from a pool of candidates. The transmitted signal from antenna p is created by concatenating all time-domain vectors broadcasted in different time slots, $\bar{\mathbf{c}}_{\varpi^{(k)}}^{(k,p)} = \left[\mathbf{c}_0^{(k,p)}, \cdots, \mathbf{c}_{N^{(k)}}^{(k,p)}\right]$, where $N^{(k)} = Z^{(k)} Z_1^{(k)} / Z_2^{(k)}$ and $\bar{\mathbf{c}}_{\varpi^{(k)}}^{(k,p)}$ is related to $\mathbf{x}^{(k)}$ through the specific structure of $\varpi^{(k)}$. Note that we attach $\varpi^{(k)}$ to $\bar{\mathbf{c}}_{\varpi^{(k)}}^{(k,p)}$ as a subscript to emphasize that the structure of vector $\bar{\mathbf{c}}_{\varpi^{(k)}}^{(k,p)}$ depends on STBC $\varpi^{(k)}$. Finally, each transmit antenna of user k communicates with the BS through unknown L-path wireless channel, $\mathbf{h}^{(k,p)} = \left[h^{(k,p)}(0), \cdots, h^{(k,p)}(L-1)\right]$.

B. RECEIVER

Because users are placed at different positions from the BS, their received signals are subjected to distinct propagation delays. The propagation delay of each user is divided into an integer part and a fractional part with respect to the sampling interval. The fractional part can be involved into the channel impulse response (CIR) of each user as reported in [28], therefore, it does not be included in the following analysis. Denoting $\mu^{(k)}$ as the integer part of the propagation delay of user k, the received signal at the BS is expressed as

$$\mathbf{r}' = \sum_{k=0}^{K-1} \sum_{p=0}^{P^{(k)}-1} \underline{\mathbf{c}}_{\varpi^{(k)}}^{(k,p)}\left(\mu^{(k)}\right) \odot \mathbf{h}^{(k,p)} + \mathbf{w}', \quad (5)$$

where $\underline{\mathbf{c}}_{\varpi^{(k)}}^{(k,p)} = \left[\mathbf{0}_{1\times\mu^{(k)}} \bar{\mathbf{c}}_{\varpi^{(k)}}^{(k,p)}\right]$ with $\mathbf{0}_{1\times\mu^{(k)}}$ being all zero sequence of length $\mu^{(k)}$, $\odot$ refers to the convolution operation, and $\mathbf{w}'$ is the corresponding additive white Gaussian noise (AWGN). The aim is to utilize the received signal $\mathbf{r}$ to identify the type of STBC $\varpi^{(k)}$ under unavailability of $\mathbf{h}^{(k,p)}$ and propagation delay $\mu^{(k)}$ for $k = 0, \cdots, K-1$, and $p = 0, \cdots, P^{(k)}-1$. This is a prerequisite for performing multi-user data detection.

III. PROPOSED ALGORITHM

For the sake of mathematical convenience, the expression of (5) is written in a matrix form as

$$\mathbf{r} = \sum_{k=0}^{K-1} \sum_{p=0}^{P^{(k)}-1} \bar{\mathbf{C}}_{\varpi^{(k)}}^{(k,p)}\left(\mu^{(k)}\right) \mathbf{h}^{(k,p)} + \mathbf{w}, \quad (9)$$

where $\mathbf{r} = \mathbf{r}'^T$ and $\mathbf{w} = \mathbf{w}'^T$. Here $(\cdot)^T$ refers to vector transpose operator and $\bar{\mathbf{C}}^{(k,p)}\left(\mu^{(k)}\right)$ is given as

$$\bar{\mathbf{C}}_{\varpi^{(k)}}^{(k,p)}\left(\mu^{(k)}\right) = \begin{bmatrix} \mathbf{0}_{\mu^{(k)}\times(L-1)} \\ \mathbf{C}_{\varpi^{(k)}}^{(k,p)} \\ \mathbf{0}_{(\mu_{\max}-\mu^{(k)}+L-1)\times(L-1)} \end{bmatrix}, \quad (10)$$

where $\mu_{\max}$ is the maximum possible integer propagation delay,[1] $\mathbf{0}_{\nu_1\times\nu_2}$ is all-zero matrix of size $\nu_1 \times \nu_2$, and $\mathbf{C}_{\varpi^{(k)}}^{(k,p)}$ is an $\left((\mathcal{M}+\nu)Z^{(k)}+L-1\right)\times(L-1)$ matrix created as

$$\mathbf{C}_{\varpi^{(k)}}^{(k,p)}(\nu_1,\nu_2) = \begin{cases} \bar{\mathbf{c}}_{\varpi^{(k)}}^{(k,p)}(\nu_1-\nu_2) \\ \text{for } \nu_1 = 0,\cdots,(\mathcal{M}+\nu)Z^{(k)}+L-1, \\ \text{and } \nu_2 = 0,\cdots,L-1,\ \nu_1 \geq \nu_2 \\ 0 \qquad\qquad \text{otherwise,} \end{cases} \quad (11)$$

where $\mathbf{C}_{\varpi^{(k)}}^{(k,p)}(\nu_1,\nu_2)$ is the element located at row ν_1 and column ν_2 of matrix $\mathbf{C}_{\varpi^{(k)}}^{(k,p)}$ and $\bar{\mathbf{c}}_{\varpi^{(k)}}^{(k,p)}(\nu_1-\nu_2)$ is the $(\nu_1-\nu_2)$th element of vector $\bar{\mathbf{c}}_{\varpi^{(k)}}^{(k,p)}$.

Bearing in mind (9), one writes the ML estimates of the unknown parameters as shown in (6), (7), and (8), as shown at the bottom of the next page. Here $\tilde{\diamond}$ is the trial value of variable $\diamond$ and $\Pr(\circ|\diamond)$ is the probability density function of $\circ$ given $\diamond$. A closer look at (7) reveals that the ML algorithm performs averaging over the transmission matrices of all users. This is because the original data symbols are unknown at the BS. However, the real implementation of (7) is not possible because it demands huge computations, which are highly undesirable in practical systems.

The expectation-maximization (EM) procedure is useful in this context as it provides a iterative technique to estimate the ML solution in the presence of nuisance parameters. The procedure updates all unknown variables simultaneously, resulting in a time-consuming and complicated search procedure due to the large number of dimensions involved. In contrast, the SAGE methodology separates the unknown variables into numerous non-overlapping groups and then utilizes the EM algorithm to modify each group one at a time. Thus, the SAGE technique can be thought of as an upgraded version of the EM algorithm, which improves the convergence rate significantly with preserving the advantages of numerical simplicity and stability. The SAGE approach has been widely utilized to tackle parameter estimate problems in multicarrier systems, such as synchronization and channel

[1] In practice, $\mu_{\max}$ is expressed as $\mu_{\max} \approx \frac{\text{cell radius}}{\text{speed of light}}$. Since $\mu_{\max}$ does not depend on users locations, user superscript k is dropped from $\mu_{\max}$ without the loss of generality.

estimation [27], [28]. It is the first time that the SAGE algorithm has been utilized to identify STBC for uplink SC-FDMA systems using channel coding outputs, which is a departure from its traditional context of parameter estimation with uncoded transmissions.

Each iteration of SAGE comprises of cycles rather than estimating all parameters at once. By maximizing the conditional expectation of the log-likelihood of the augmented data corresponding to a cycle, the parameter subset associated with this cycle is updated. As a result, the complex multidimensional search problem that is required to maximize the likelihood function is reduced to several one-dimensional effortless search problems.

The mathematical details of the proposed SAGE procedure for computing the parameters under consideration are provided as follows. We divide the unknown parameters into K non-overlapping subgroups $\left\{\left[\varpi^{(0)}, \mu^{(0)}, \mathbf{h}^{(0,p^{(0)})}\right], \cdots, \left[\varpi^{(K-1)}, \mu^{(K-1)}, \mathbf{h}^{(K-1,p^{(K-1)})}\right]\right\}$. A single user's parameters are updated at a time. This means that an iteration is made up of K cycles, each of which updates the user's settings. Given initial estimates, the $(\iota+1)$th iteration consists of the following steps.

- During the k'th cycle, we update the parameters of user k' while the other users' parameters remain unaltered.
- Subtracting all other users' MAI from the total received signal produces

$$\mathbf{y}_{k'} = \mathbf{r} - \sum_{k=0,\, k\neq k'}^{K-1} \sum_{p=0}^{\hat{P}^{(k)(\iota)}-1} \Omega^{(k,p)}\left(\hat{\varpi}^{(k)}(\iota), \hat{\mu}^{(k)}(\iota)\right) \hat{\mathbf{h}}^{(k,p)}(\iota), \tag{14}$$

where $\mathbf{y}_{k'}$ is the received signal ingredient of user k', $\Omega^{(k,p)}\left(\hat{\varpi}^{(k)}(\iota), \hat{\mu}^{(k)}(\iota)\right)$ is the a posteriori expectation of the transmission matrix $\bar{\mathbf{C}}^{(k,p)}_{\hat{\varpi}^{(k)}(\iota)}\left(\mu^{(k)}\right)$ given in (10), and $\hat{P}^{(k)}(\iota)$, $\hat{\varpi}^{(k)}(\iota)$, $\hat{\mu}^{(k)}(\iota)$ and $\hat{\mathbf{h}}^{(k,p)}(\iota)$ are the estimates of $P^{(k)}$, $\varpi^{(k)}$, $\mu^{(k)}$, and $\mathbf{h}^{(k,p)}$, respectively, at iteration ι. Note that $\bar{\mathbf{C}}^{(k,p)}_{\hat{\varpi}^{(k)}(\iota)}\left(\hat{\mu}^{(k)}(\iota)\right)$ is inaccessible since the sent information are unknown at the BS. As a result, $\Omega^{(k,p)}\left(\hat{\varpi}^{(k)}(\iota), \hat{\mu}^{(k)}(\iota)\right)$ is used in (14) instead of $\bar{\mathbf{C}}^{(k,p)}_{\hat{\varpi}^{(k)}(\iota)}\left(\mu^{(k)}\right)$. Mathematically, $\Omega^{(k,p)}\left(\hat{\varpi}^{(k)}(\iota), \hat{\mu}^{(k)}(\iota)\right)$ is expressed as

$$\Omega^{(k,p)}\left(\hat{\varpi}^{(k)}(\iota), \hat{\mu}^{(k)}(\iota)\right) = \mathrm{E}\left[\bar{\mathbf{C}}^{(k,p)}_{\hat{\varpi}^{(k)}(\iota)}\left(\hat{\mu}^{(k)}(\iota)\right) \middle| \mathbf{y}_k, \hat{\mathbf{h}}^{(k,p)}(\iota)\right], \tag{15}$$

where $\mathrm{E}[\cdot]$ is the statistical expectation over the transmitted data symbols of user k. One rewrites (15) as

$$\begin{aligned}\Omega\left(\hat{\varpi}^{(k)}(\iota), \hat{\mu}^{(k)}(\iota)\right) &= \int \bar{\mathbf{C}}^{(k,p)}_{\hat{\varpi}^{(k)}(\iota)}\left(\hat{\mu}^{(k)}(\iota)\right) \\ &\quad \times \Pr\left(\bar{\mathbf{C}}^{(k,p)}_{\hat{\varpi}^{(k)}(\iota)}\left(\hat{\mu}^{(k)}(\iota)\right) \middle| \mathbf{y}_k, \hat{\mathbf{h}}^{(k,p)}(\iota)\right) \\ &\quad \times d\bar{\mathbf{C}}^{(k,p)}_{\hat{\varpi}^{(k)}(\iota)}\left(\hat{\mu}^{(k)}(\iota)\right).\end{aligned} \tag{16}$$

- To compute the updated values of the parameter set of user k', we describe the log-likelihood function as

$$\mathcal{L} = \log \Pr\left(\mathbf{y}_{k'} \middle| \bar{\mathbf{C}}^{(k',p)}_{\varpi^{(k')}}\left(\mu^{(k')}\right), \mathbf{h}^{(k',p)}\right). \tag{17}$$

Bearing in mind that

$$\Pr\left(\mathbf{y}_{k'} \middle| \bar{\mathbf{C}}^{(k',p)}_{\varpi^{(k')}}\left(\mu^{(k')}\right), \mathbf{h}^{(k,p)}\right) \propto \exp\left(\frac{-1}{\sigma_n^2} \sum_{p=0}^{P^{(k')-1}} \left\| \mathbf{y}_{k'} - \bar{\mathbf{C}}^{(k',p)}_{\varpi^{(k')}}\left(\mu^{(k')}\right) \mathbf{h}^{(k',p)} \right\|^2\right), \tag{18}$$

$$\left[\hat{\varpi}^{(0)}, \cdots, \hat{\varpi}^{(K-1)}, \hat{\mu}^{(0)}, \cdots, \hat{\mu}^{(K-1)}, \hat{\mathbf{h}}^{(0,0)}, \cdots, \hat{\mathbf{h}}^{(K-1,P^{(K-1)})}\right] = \underset{\tilde{\varpi}^{(0)}, \cdots, \tilde{\varpi}^{(K-1)}, \tilde{\mu}^{(0)}, \cdots, \tilde{\mu}^{(K-1)}, \tilde{\mathbf{h}}^{(0,0)}, \cdots, \tilde{\mathbf{h}}^{(K-1,P^{(K-1)})}}{\arg\max} \Pr\left(\mathbf{r} \middle| \tilde{\varpi}^{(0)}, \tilde{\mu}^{(0)}, \tilde{\mathbf{h}}^{(0,0)}, \cdots, \tilde{\varpi}^{(K-1)}, \tilde{\mu}^{(K-1)}, \tilde{\mathbf{h}}^{(K-1,P^{(K-1)})}\right), \tag{6}$$

where,

$$\Pr\left(\mathbf{r} \middle| \tilde{\varpi}^{(0)}, \tilde{\mu}^{(0)}, \tilde{\mathbf{h}}^{(0,0)}, \cdots, \tilde{\varpi}^{(K-1)}, \tilde{\mu}^{(K-1)}, \tilde{\mathbf{h}}^{(K-1,P^{(K-1)})}\right) \propto \sum_{\tilde{\mathbf{C}}^{(0,0)}_{\tilde{\varpi}^{(0)}}(\tilde{\mu}^{(0)}), \cdots, \tilde{\mathbf{C}}^{(K-1,P^{(K-1)})}_{\tilde{\varpi}^{(K-1)}}(\tilde{\mu}^{(K-1)})} \Pr\left(\mathbf{r} \middle| \tilde{\mathbf{C}}^{(0,0)}_{\tilde{\varpi}^{(0)}}\left(\tilde{\mu}^{(0)}\right), \tilde{\mathbf{h}}^{(0,0)}, \cdots, \tilde{\mathbf{C}}^{(K-1,P^{(K-1)})}_{\tilde{\varpi}^{(K-1)}}\left(\tilde{\mu}^{(K-1)}\right), \tilde{\mathbf{h}}^{(K-1,P^{(K-1)})}\right), \tag{7}$$

and

$$\Pr\left(\mathbf{r} \middle| \tilde{\mathbf{C}}^{(0,0)}_{\tilde{\varpi}^{(0)}}\left(\tilde{\mu}^{(0)}\right), \tilde{\mathbf{h}}^{(0,0)}, \cdots, \tilde{\mathbf{C}}^{(K-1,P^{(K-1)})}_{\tilde{\varpi}^{(K-1)}}\left(\tilde{\mu}^{(K-1)}\right), \tilde{\mathbf{h}}^{(K-1,P^{(K-1)})}\right) \propto \exp\left(\frac{-1}{\sigma_n^2} \sum_{k=0}^{K-1} \sum_{p=0}^{P^{(K-1)}} \left\| \mathbf{r} - \tilde{\mathbf{C}}^{(k,p)}_{\tilde{\varpi}^{(k)}}\left(\tilde{\mu}^{(k)}\right) \tilde{\mathbf{h}}^{(k,p)} \right\|^2\right). \tag{8}$$

then, after eliminating the useless elements, we rewrite (17) as

$$\mathcal{L} \propto 2 \sum_{p=0}^{P^{(k')}-1} \left\{ \Re \left(\mathbf{y}_{k'}^{H} \bar{\mathbf{C}}_{\varpi^{(k')}}^{(k',p)} \left(\mu^{(k')} \right) \mathbf{h}^{(k',p)} \right) - \mathbf{h}^{(k',p)H} \bar{\mathbf{C}}_{\varpi^{(k')}}^{(k',p)} \left(\mu^{(k')} \right)^{H} \bar{\mathbf{C}}_{\varpi^{(k')}}^{(k',p)} \left(\mu^{(k')} \right) \mathbf{h}^{(k',p)} \right\}. \tag{19}$$

- In the EM processor's expectation step, given the existing estimates, the expected value of $\mathcal{L}$ with regard to transmitted data symbols is calculated in (12), as shown at the bottom of the page, where $\Re(\cdot)$ denotes the real value of a complex argument.
- In the EM processor's maximization step, the parameters of user k' is updated as indicated in (13), as shown at the bottom of the page. To simplify the multidimensional optimization problem shown in (13), we decompose the joint problem into simple dimensional search problems as follows. For each discrete pair of $\left(\mu^{(k')}, \varpi^{(k')}\right)$, the updated value of $\mathbf{h}^{(k',p)}$ is computed by setting the derivative of the objective function in (12) to zero as

$$\hat{\mathbf{h}}^{(k',p)}(\iota+1) = \left(\Omega^{H} \left(\mu^{(k')}, \varpi^{(k')} \right) \Omega \left(\mu^{(k')}, \varpi^{(k')} \right) \right)^{-1} \times \Omega^{H} \left(\mu^{(k')}, \varpi^{(k')} \right) \mathbf{y}_{k'}. \tag{20}$$

Using (20) into (12), the updated values of $\mu^{(k')}$ and $\varpi^{(k')}$ are computed as

$$\left[\hat{\varpi}^{(k')}(\iota+1), \hat{\mu}^{(k')}(\iota+1) \right] = \arg\max_{\varpi^{(k')}, \mu^{(k')}} \sum_{p=0}^{P^{(k')}-1} \left\{ 2\Re \left(\mathbf{y}_{k'}^{H} \Omega \left(\mu^{(k')}, \varpi^{(k')} \right) \hat{\mathbf{h}}^{(k',p)}(\iota+1) \right) - \hat{\mathbf{h}}^{(k',p)H}(\iota+1) \Omega^{H} \left(\mu^{(k')}, \varpi^{(k')} \right) \times \Omega \left(\mu^{(k')}, \varpi^{(k')} \right) \hat{\mathbf{h}}^{(k',p)}(\iota+1) \right\}. \tag{21}$$

IV. PRACTICAL CONSIDERATIONS AND INTERPRETATIONS

The following practical concerns with the suggested iterative identification, estimation, and data detection structure are worth mentioning.

A. EXPECTATION OF TRANSMISSION MATRICES

As observed from (15), (20), and (21), the proposed design relies on determining the expectation of each user's transmission matrix $\Omega\left(\hat{\varpi}^{(k)}(\iota), \hat{\mu}^{(k)}(\iota)\right)$. How to compute this matrix in practice is a question that emerges. According to (15), $\Omega^{(k,p)}\left(\hat{\varpi}^{(k)}(\iota), \hat{\mu}^{(k)}(\iota)\right)$ can be calculated by substituting each matrix element with its a posteriori expectation. Bearing (4) in mind, the a posteriori expectation of transmitted sample $x_z^{(k)}(m_1)$ is expressed as

$$\mathrm{E}\left[x_z^{(k)}(m_1) \left| \mathbf{y}_k, \hat{\varpi}^{(k)}(\iota), \hat{\mu}^{(k)}(\iota) \right. \right] = \sum_{m_2=0}^{\mathcal{M}-1} \mathrm{E}\left[\tilde{d}_z^{(k)}(m_2) \left| \mathbf{y}_k, \hat{\varpi}^{(k)}(\iota), \hat{\mu}^{(k)}(\iota) \right. \right] \times \exp\left(j2\pi m_1 m_2/\mathcal{M}\right), \tag{22}$$

where

$$\mathrm{E}\left[\tilde{d}_z^{(k)}(m_2) \left| \mathbf{y}_k, \hat{\varpi}^{(k)}(\iota), \hat{\mu}^{(k)}(\iota) \right. \right] = \sum_{\tilde{d}_z^{(k)}(m_2) \in \Phi^{(k)}} \tilde{d}_z^{(k)}(m_2) \Pr\left(\tilde{d}_z^{(k)}(m_2) \left| \mathbf{y}_k, \hat{\varpi}^{(k)}(\iota), \hat{\mu}^{(k)}(\iota) \right. \right). \tag{23}$$

As noted from (23), the key issue is to compute the a posteriori probability of $\Pr\left(\tilde{d}_z^{(k)}(m_2) \left| \mathbf{y}_k, \hat{\varpi}^{(k)}(\iota), \hat{\mu}^{(k)}(\iota) \right.\right)$. Fortunately, the decoders of modern error-correcting codes include convolutional, turbo, and low-density parity check codes computes this probability during their iterative nature [32], [33]. As a result, we exploit this probability to support the proposed identification and estimation algorithm without causing extra overhead on the decoding process. The conceptual block diagram of the proposed design is shown in figure 2.

B. CHANNEL DECODER UPDATE

We must re-compute $\Pr\left(\tilde{d}_z^{(k)}(m_2) \left| \mathbf{y}_k, \hat{\varpi}^{(k)}(\iota), \hat{\mu}^{(k)}(\iota) \right.\right)$ every time we update $\varpi^{(k)}(\iota)$, $\mu^{(k)}(\iota)$, and $\mathbf{h}^{(k,p)}$ for every user k. This necessitates the resetting of the channel decoder, which results in numerous iterations. To reduce this overhead, we employ the embedded estimation technique [34], in which the channel decoder isn't rebooted when the parameters $\varpi^{(k)}(\iota)$, $\mu^{(k)}(\iota)$, and $\mathbf{h}^{(k,p)}$ are updated, but the extrinsic and a priori probabilities from the previous iteration of the channel decoder are kept unchanged. The overhead associated

$$Q\left(\varpi^{(k')}, \mu^{(k')}, \mathbf{h}^{(k',0)}, \cdots, \mathbf{h}^{(k',P^{(k')}-1)} \left| \hat{\varpi}^{(k')}(\iota), \hat{\mu}^{(k')}(\iota), \hat{\mathbf{h}}^{(k,0)}(\iota), \cdots, \hat{\mathbf{h}}^{(k,\hat{P}^{(k')}(\iota)-1)}(\iota) \right. \right) \propto \sum_{p=0}^{P^{(k')}-1} \left\{ 2\Re \left(\mathbf{y}_{k'}^{H} \Omega \left(\mu^{(k')}, \varpi^{(k')} \right) \mathbf{h}^{(k',p)} \right) - \mathbf{h}^{(k',p)H} \Omega^{H} \left(\mu^{(k')}, \varpi^{(k')} \right) \Omega \left(\mu^{(k')}, \varpi^{(k')} \right) \mathbf{h}^{(k',p)} \right\} \tag{12}$$

$$\left[\hat{\varpi}^{(k')}(\iota+1), \hat{\mu}^{(k')}(\iota+1), \hat{\mathbf{h}}^{(k',0)}(\iota+1), \cdots, \hat{\mathbf{h}}^{\left(k',P^{(k')}-1\right)}(\iota+1) \right] = \arg\max_{\varpi^{(k')}, \mu^{(k')}, \mathbf{h}^{(k',0)}, \cdots, \mathbf{h}^{(k',P^{(k')}-1)}} Q\left(\varpi^{(k')}, \mu^{(k')}, \mathbf{h}^{(k',0)}, \cdots, \mathbf{h}^{(k',P^{(k')}-1)} \left| \hat{\varpi}^{(k')}(\iota), \hat{\mu}^{(k')}(\iota), \hat{\mathbf{h}}^{(k,0)}(\iota), \cdots, \hat{\mathbf{h}}^{(k,\hat{P}^{(k')}(\iota)-1)}(\iota) \right. \right) \tag{13}$$

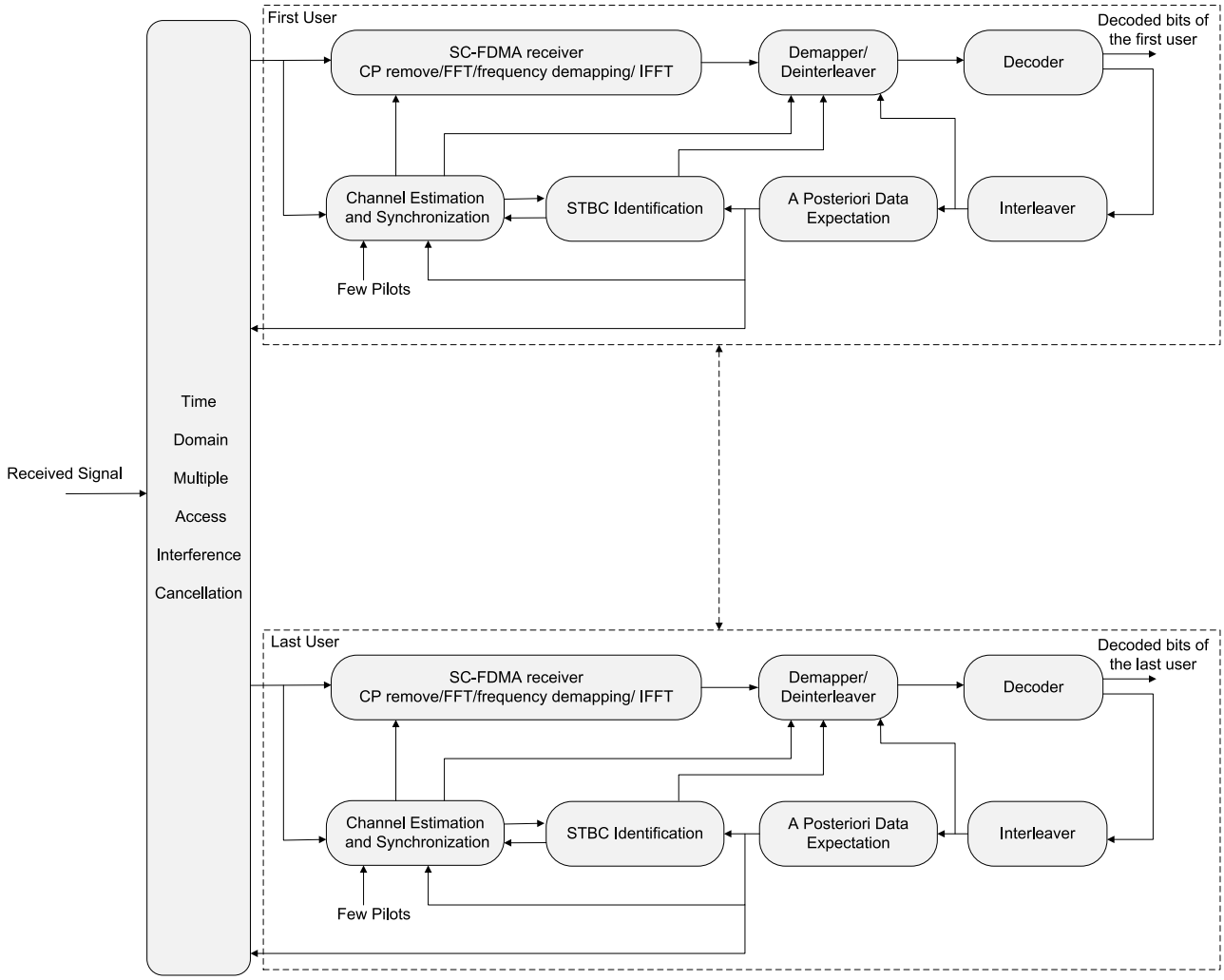

FIGURE 2. Conceptual block diagram of the proposed design at BS.

TABLE 1. Processing complexity per iteration.

Equation	Required flops
Channel update (20)	$16\lambda\,(L-1)^2+8\,(L-1)^3+8\lambda\,(L-1)$
Code and synchronization update (21)	$8\mu_{max}\mathcal{Z}(L-1)(M+2)$

with the suggested iterative procedure becomes tolerable in this instance.

C. PROCESSING COMPLEXITY

We analyze the processing complexity of the proposed SAGE-based identification algorithm in terms of the number of floating operations (fps). Using the same methodology as previously detailed in [35], [36], the precise computations of the required computational complexity ψ per iteration per user is

$$\psi = 16\lambda\,(L-1)^2+8\,(L-1)^3+8\lambda\,(L-1) \\ +8\mu_{max}\mathcal{Z}(L-1)(\lambda+2), \quad (24)$$

where $\lambda=(\mathcal{M}+\nu)\,g+L-1$ with g being the maximum number of input STBC blocks and $\mathcal{Z}$ is the number of STBC candidates. Table 1 outlines the specific stages involved in the calculations. For example, we consider system specifications of $\mathcal{M}=1024$, $\nu=7$, $g=10$, $L=6$, $\mu_{max}=30$, $\mathcal{Z}=5$. This provides $8.3(10)^6$ fps, which yields a run-time of 66.4 μsec with a central processing unit of 1 Terafps per second [3]. This run-time is clearly appropriate in terms of actual execution.

D. INITIAL ESTIMATES

Users send a few pilot symbols to the BS in order to initialize the proposed SAGE-based algorithm. As the number of pilot

symbols grows, the first estimates $\hat{\varpi}^{(k)}(0)$, $\hat{\mu}^{(k)}(0)$, and $\hat{\mathbf{h}}^{(k,p)}(0)$ improve. Increasing the number of pilot symbols, on the other hand, reduces the amount of energy available for data symbols and increases the needed bandwidth. As a result, the number of pilot symbols to data symbols must be remain as low as feasible. In the sense that it produces good identification performance with minimal throughput loss, the suggested algorithm takes advantage of the data symbols' soft information supplied by the channel decoders. Without the use of supplemental pilot symbols, this iteratively improves the first estimates. The starting values of $\hat{\varpi}^{(k)}(0)$, $\hat{\mu}^{(k)}(0)$, and $\hat{\mathbf{h}}^{(k,p)}(0)$ are extracted from (15) by setting the entries in $\Omega\left(\mu^{(k)}, \varpi^{(k)}\right)$ to simply the contribution of pilot symbols.

V. SIMULATION RESULTS

The proposed STBC identification technique was investigated using Monte Carlo simulations. If not stated differently, we considered a SC-FDMA system with the following parameters.

- The number of active users was $K = 8$.
- The number of total subcarriers was $\mathcal{M} = 1024$.
- The number of allocated subcarriers per user was $M_s = 128$.
- The number of cyclic prefix samples was $\nu = 16$.
- The interleaved sub-carrier assignment was used.
- The allocated signal constellation $\Phi^{(k)}$ for each user was randomly selected from a pool of eight higher order QAM constellations, 4-QAM, 8-QAM, 16-QAM, ..., 512-QAM. Similar results can be accomplished with ease for PSK signals.
- A convolutional code of rate 1/2, constraint length 5, and generator polynomials $(23)_8$ and $(35)_8$ was employed for each user.
- Pilot symbols of length $P_s = 40$ were inserted to initialize the identification process.
- Each wireless channel, $\mathbf{h}^{(k,p)}$ between antenna p of user k and the BS was generated using 15 paths where each one has an exponential power delay profile as [24], [37]:

$$\sigma_{ch}^2(l) = \Xi_{ch} \exp(-l/10), \; l = 0, \ldots, 14 \tag{25}$$

  where Ξ_{ch} was selected in such a way that the average energy was equal to one.
- The maximum propagation delay normalized to the sampling duration was $\mu_{max} = 50$, and each user's propagation delay was chosen at random.
- Each user was assigned an STBC at random from the list of {ST1, ST2, ST3, ST4, ST5} where those candidates' transmission matrices are shown in (26a-26e) [15], [22]. It is worth mentioning that the proposed identifier can be employed with any number of STBCs. Those five codes are offered solely for the purpose of simulating various scenarios.

$$\text{ST1}(x_0, x_1) = [x_0, x_1]^T, \tag{26a}$$

$$\text{ST2}(x_0, x_1) = \begin{bmatrix} x_0 & x_1 \\ -x_1^* & x_0^* \end{bmatrix}^T, \tag{26b}$$

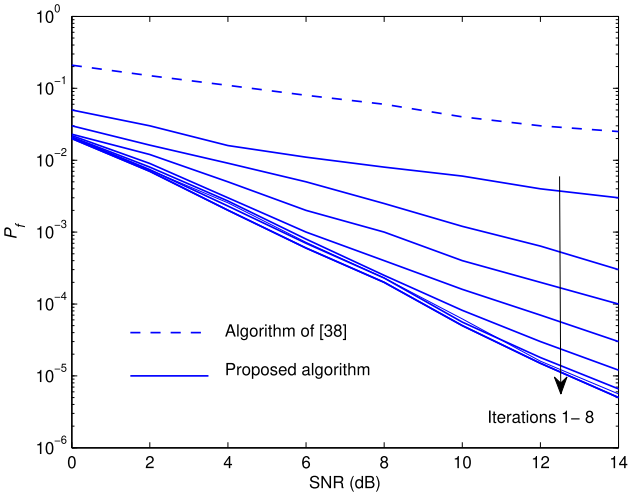

FIGURE 3. Comparison of identification performance between the proposed algorithm and the algorithm presented in [38] for single-user transmission ($K = 1$), code set = {SM, AL}.

$$\text{ST3}(x_0, x_1, x_2) = \begin{bmatrix} x_0 & x_1 & x_2 \\ -x_1^* & x_0^* & 0 \\ x_2^* & 0 & -x_0^* \\ 0 & -x_2^* & x_1^* \end{bmatrix}^T, \tag{26c}$$

$$\text{ST4}(x_0, x_1, x_2) = \begin{bmatrix} x_0 & x_1 & \frac{x_2}{\sqrt{2}} \\ -x_1^* & x_0^* & \frac{x_2}{\sqrt{2}} \\ \frac{x_2^*}{\sqrt{2}} & \frac{x_2^*}{\sqrt{2}} & \frac{-x_0-x_0^*+x_1-x_1^*}{2} \\ \frac{x_2^*}{\sqrt{2}} & -\frac{x_2^*}{\sqrt{2}} & \frac{x_1+x_1^*+x_0-x_0^*}{2} \end{bmatrix}^T, \tag{26d}$$

$$\text{ST5}(x_0, x_1, x_2, x_3) = \begin{bmatrix} x_0 & x_1 & x_2 & x_3 \\ -x_1 & x_0 & -x_3 & x_2 \\ -x_2 & x_3 & x_0 & -x_1 \\ -x_3 & -x_2 & x_1 & x_0 \\ x_0^* & x_1^* & x_2^* & x_3^* \\ -x_1^* & x_0^* & -x_3^* & x_2^* \\ -x_2^* & x_3^* & x_0^* & -x_1^* \\ -x_3^* & -x_2^* & x_1^* & x_0^* \end{bmatrix}^T. \tag{26e}$$

- The probability of incorrect identification P_f was utilized as a figure of merit for the suggested identifier, probability mass function P_m was employed to evaluate the proposed synchronizer, and the mean square estimation error (MSE) was used to assess channel estimation performance.

Figure 3 compares the STBC identification performance of the proposed algorithm to that of [38] for a single-user transmission over a wide range of signal-to-noise ratios (SNR). As far as the authors' knowledge, the mentioned reference is the sole study in the literature dedicated to STBC identification for SC-FDMA systems, and it is restricted to the classification of AL and SM STBC signals over a single-user transmission. To be fair, the proposed algorithm's identification performance is also limited to these signals. As can be observed, the proposed algorithm's identification improves

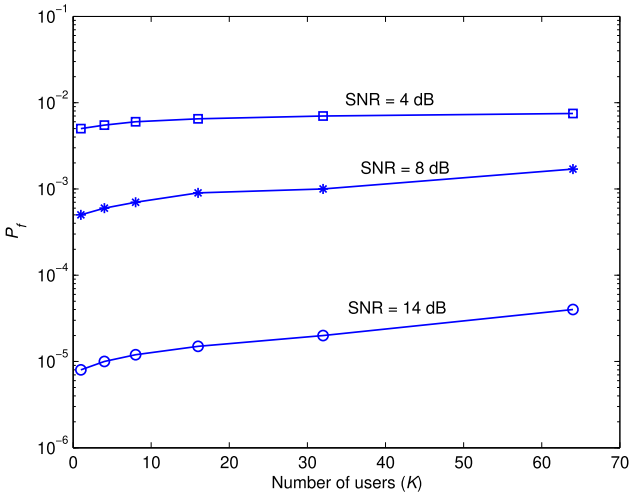

FIGURE 4. Identification performance of the proposed algorithm as a function of the number of users at different SNR values. The number of iterations is seven and STBC set is {ST1, ST2, ST3, ST4, ST5}.

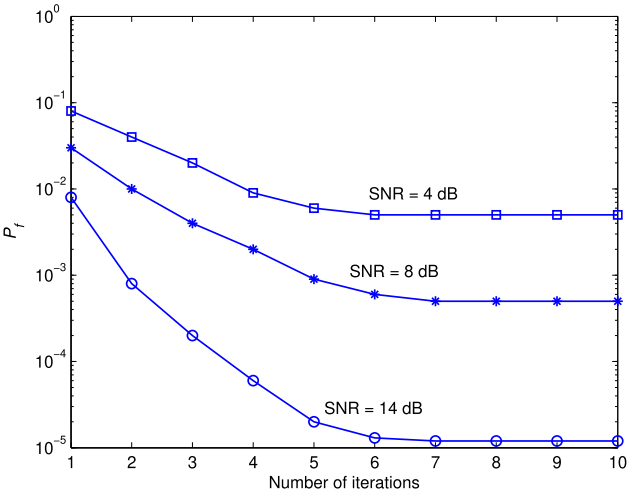

FIGURE 5. Identification performance of the proposed algorithm as a function of the number of iterations at different SNR values. The number of user is eight and STBC set is {ST1, ST2, ST3, ST4, ST5}.

with iterations. This is in line with the theoretical analysis presented in Section III. Furthermore, the suggested approach significantly outperforms [38]. This is due to the fact that we employ the channel decoder outputs to refine the identification process, whereas [38] does not.

Figure 4 describes the proposed algorithm's STBC identification performance as a function of the number of users at different values of SNR, with the number of iterations being seven. Hereafter, each user selects a STBC signal among the five candidates shown in (26a-26e). It is worth noting that the values of P_f at $K = 1$ of this figure are slightly greater than that in the preceding one. This is due to the fact that we are classifying among five STBC signals in this figure. However, in the prior one, we were limited to only two STBC signals. It has been observed from figure 4 that there is a performance loss in P_f when compared to a single-user transmission. This is the result of MAI associated with the circumstance of multiple users. Despite the fact that we developed a method to eliminate this interference as indicated in (14). This deterioration, which is caused by residual interference, has a slight detrimental influence at high values of SNR and a large number of users. However, it almost vanishes otherwise. This is due to the fact that in the former case, the residual interference dominates with a lesser influence of AWGN.

In order to access iterative algorithm's convergence rate, figure 5 evaluates the identification performance as a function of the number of iterations for eight users at different values of SNR. In general, the number of iterations required to reach convergence depends on many factors such as the operating SNR, number of active users, number of pilots, and the type of the channel coding used. More iterations are needed when the initial values are far away from the actual values. Figure 5 concludes that the proposed iterative structure is essentially converged at 7 iterations at most.

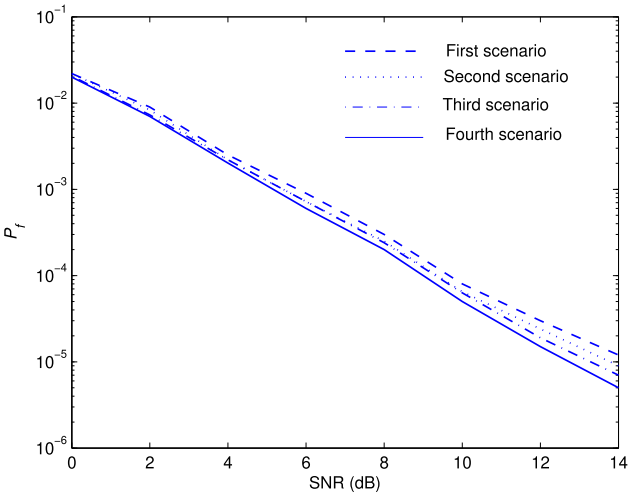

FIGURE 6. Identification performance of the proposed design in four scenarios at iteration 7, $K = 8$.

Figure 6 depicts the identification performance of the proposed design in four scenarios at iteration 7. The first scenario includes STBC identification as well as propagation delays and channel impulse responses estimation. The second one involves STBC identification and channel estimation with perfect estimation of propagation delays. Third scenario performs STBC identification and propagation delays with perfect channel estimation. The last one has STBC identification with perfect estimation of propagation delays and channel impulse responses. The results show that there are no significant variations in the identification performance of the four scenarios. This validates the proposed STBC identification algorithm with channel estimates for asynchronous uplink SC-FDMA transmissions.

The mean square error of the proposed channel estimator is shown in Figure 7 as a function of SNR and the number of iterations. The MSE performance is low in the initialization step. However, by utilizing soft information of channel

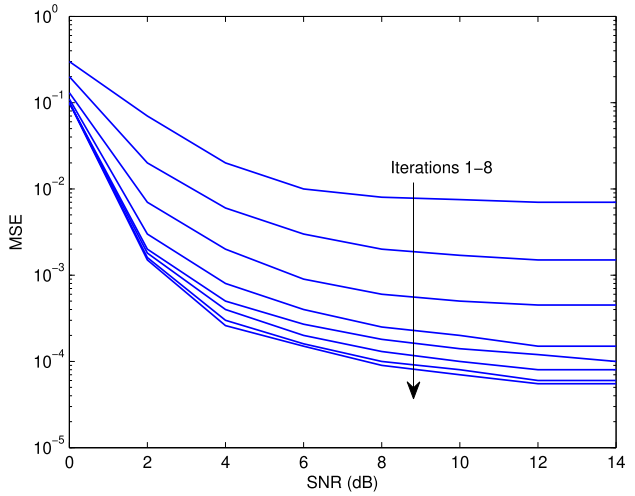

FIGURE 7. MSE of the proposed channel estimator.

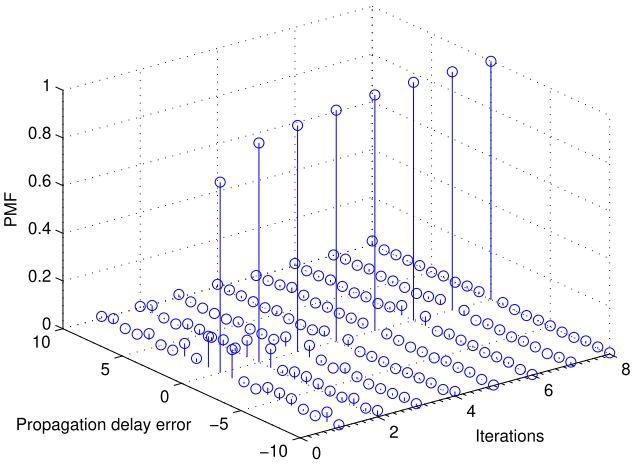

FIGURE 8. PMF of the propagation delay error of the proposed synchronizer at SNR = 14 dB.

decodes as mentioned in (20), the suggested estimator's performance improves until it converges at the seventh iteration.

Figure 8 illustrates the probability mass function of the propagation delay error, $\tau_\Delta = \frac{1}{K}\sum_{k=0}^{K-1}\left(\varpi^{(k)} - \hat{\varpi}^{(k)}\right)$, of the proposed synchronizer at SNR = 14 dB. As previously explained, the performance improves with iterations. This is consistent with the theoretical conclusions in Section III.

VI. CONCLUSION

This work investigated the problem of space-time block coding (STBC) identification for multi-user uplink asynchronous transmissions in single-carrier frequency division multiple access (SC-FDMA) systems. The mathematical analysis revealed that a space-alternating expectation-maximization (SAGE) approach can be used to implement the maximum-likelihood (ML) solution of STBC identification, channel estimation, and synchronization. The channel decoder's a posteriori probabilities were exploited to improve the quality of identification and estimation processes in an iterative manner. Simulation results indicated that the proposed design outperforms the existing identification algorithms reported in the literature, with a reasonable processing time. Despite the fact that the presented strategy has recognized to be an effective technique for STBC identification, it is constrained by the requirements of the modulation type and error correcting codes being used. The process of jointly identifying all of these factors will be undertaken in the future.

ACKNOWLEDGMENT

Princess Nourah bint Abdulrahman University Researchers Supporting Project number (PNURSP2022R137), Princess Nourah bint Abdulrahman University, Riyadh, Saudi Arabia. The authors would like to acknowledge the support of Prince Sultan University for paying the Article Processing Charges (APC) of this publication.

REFERENCES

[1] A. Serbes, H. Cukur, and K. Qaraqe, "Probabilities of false alarm and detection for the first-order cyclostationarity test: Application to modulation classification," *IEEE Commun. Lett.*, vol. 24, no. 1, pp. 57–61, Jan. 2020.

[2] T. Huynh-The, Q.-V. Pham, T.-V. Nguyen, T. T. Nguyen, R. Ruby, M. Zeng, and D.-S. Kim, "Automatic modulation classification: A deep architecture survey," *IEEE Access*, vol. 9, pp. 142950–142971, 2021.

[3] M. Marey and H. Mostafa, "Turbo modulation identification algorithm for OFDM software-defined radios," *IEEE Commun. Lett.*, vol. 25, no. 5, pp. 1707–1711, May 2021.

[4] M. Marey, H. Mostafa, S. A. Alshebeili, and O. A. Dobre, "Blind modulation identification algorithm for two-path successive relaying systems," *IEEE Wireless Commun. Lett.*, vol. 10, no. 11, pp. 2369–2373, Nov. 2021.

[5] Z. Xing and Y. Gao, "A modulation classification algorithm for multipath signals based on cepstrum," *IEEE Trans. Instrum. Meas.*, vol. 69, no. 7, pp. 4742–4752, Jul. 2020.

[6] R. Gupta, S. Kumar, and S. Majhi, "Blind modulation classification for asynchronous OFDM systems over unknown signal parameters and channel statistics," *IEEE Trans. Veh. Technol.*, vol. 69, no. 5, pp. 5281–5292, May 2020.

[7] Z. Wu, L. Zhang, Z. Zhong, and R. Liu, "Blind recognition of LDPC codes over candidate set," *IEEE Commun. Lett.*, vol. 24, no. 1, pp. 11–14, Jan. 2020.

[8] T. Xia and H.-C. Wu, "Novel blind identification of LDPC codes using average LLR of syndrome *a posteriori* probability," *IEEE Trans. Signal Process.*, vol. 62, no. 3, pp. 632–640, Feb. 2014.

[9] T. Xia and H.-C. Wu, "Blind identification of nonbinary LDPC codes using average LLR of syndrome *a posteriori* probability," *IEEE Commun. Lett.*, vol. 17, no. 7, pp. 1301–1304, Jul. 2013.

[10] R. Swaminathan and A. S. Madhukumar, "Classification of error correcting codes and estimation of interleaver parameters in a noisy transmission environment," *IEEE Trans. Broadcast.*, vol. 63, no. 3, pp. 463–478, Sep. 2017.

[11] Y. G. Debessu, H.-C. Wu, and H. Jiang, "Novel blind encoder parameter estimation for turbo codes," *IEEE Commun. Lett.*, vol. 16, no. 12, pp. 1917–1920, Dec. 2012.

[12] Y. Huang, Y. Chen, Y. T. Hou, W. Lou, and J. H. Reed, "Recent advances of LTE/WiFi coexistence in unlicensed spectrum," *IEEE Netw.*, vol. 32, no. 2, pp. 107–113, Mar. 2018.

[13] L. Wang, M. Zeng, J. Guo, Q. Cui, and Z. Fei, "Joint bandwidth and transmission opportunity allocation for the coexistence between NR-U and WiFi systems in the unlicensed band," *IEEE Trans. Veh. Technol.*, vol. 70, no. 11, pp. 11881–11893, Nov. 2021.

[14] Y. A. Eldemerdash, M. Marey, O. A. Dobre, G. K. Karagiannidis, and R. Inkol, "Fourth-order statistics for blind classification of spatial multiplexing and Alamouti space-time block code signals," *IEEE Trans. Commun.*, vol. 61, no. 6, pp. 2420–2431, Jun. 2013.

[15] M. Marey, O. A. Dobre, and R. Inkol, "Classification of space-time block codes based on second-order cyclostationarity with transmission impairments," *IEEE Trans. Wireless Commun.*, vol. 11, no. 7, pp. 2574–2584, Jul. 2012.

[16] M. Marey, O. A. Dobre, and B. Liao, "Classification of STBC systems over frequency-selective channels," *IEEE Trans. Veh. Technol.*, vol. 64, no. 5, pp. 2159–2164, May 2015.
[17] V. Choqueuse, M. Marazin, L. Collin, K. C. Yao, and G. Burel, "Blind recognition of linear space–time block codes: A likelihood-based approach," *IEEE Trans. Signal Process.*, vol. 58, no. 3, pp. 1290–1299, Mar. 2010.
[18] V. Choqueuse, K. Yao, L. Collin, and G. Burel, "Hierarchical space-time block code recognition using correlation matrices," *IEEE Trans. Wireless Commun.*, vol. 7, no. 9, pp. 3526–3534, Sep. 2008.
[19] Y. Zhang, W. Yan, L. Zhang, and L. Ma, "Automatic space-time block code recognition using convolutional neural network with multi-delay features fusion," *IEEE Access*, vol. 9, pp. 79994–80005, 2021.
[20] L. Xiao, D. Chen, I. Hemadeh, P. Xiao, and T. Jiang, "Generalized space time block coded spatial modulation for open-loop massive MIMO downlink communication systems," *IEEE Trans. Commun.*, vol. 68, no. 11, pp. 6858–6871, Nov. 2020.
[21] V. Abbasi, M. G. Shayesteh, and M. Ahmadi, "An efficient space time block code for LTE-A system," *IEEE Signal Process. Lett.*, vol. 21, no. 12, pp. 1526–1530, Dec. 2014.
[22] G. Giannakis, Z. Liu, X. Ma, and S. Zhou, *Space-Time Coding for Broadband Wireless Communications*. Hoboken, NJ, USA: Wiley, 2007.
[23] M. Marey, O. A. Dobre, and R. Inkol, "Blind STBC identification for multiple-antenna OFDM systems," *IEEE Trans. Commun.*, vol. 62, no. 5, pp. 1554–1567, May 2014.
[24] M. Marey and O. A. Dobre, "Automatic identification of space-frequency block coding for OFDM systems," *IEEE Trans. Wireless Commun.*, vol. 16, no. 1, pp. 117–128, Jan. 2017.
[25] E. Karami and O. A. Dobre, "Identification of SM-OFDM and AL-OFDM signals based on their second-order cyclostationarity," *IEEE Trans. Veh. Technol.*, vol. 64, no. 3, pp. 942–953, Mar. 2015.
[26] Y. A. Eldemerdash, O. A. Dobre, and B. J. Liao, "Blind identification of SM and Alamouti STBC-OFDM signals," *IEEE Trans. Wireless Commun.*, vol. 14, no. 2, pp. 972–982, Feb. 2015.
[27] J.-H. Lee and S.-C. Kim, "Detection of interleaved OFDMA uplink signals in the presence of residual frequency offset using the SAGE algorithm," *IEEE Trans. Veh. Technol.*, vol. 56, no. 3, pp. 1455–1460, May 2007.
[28] M. O. Pun, M. Morelli, and C. C. J. Kuo, "Iterative detection and frequency synchronization for OFDMA uplink transmissions," *IEEE Trans. Wireless Commun.*, vol. 6, no. 2, pp. 629–639, Feb. 2007.
[29] N. Iqbal, A. Zerguine, and M.-S. Alouini, "A robust frequency domain decision feedback equalization system for uplink SC-FDMA systems," *IEEE Trans. Wireless Commun.*, vol. 20, no. 12, pp. 8110–8118, Dec. 2021.
[30] N. Iqbal, N. Al-Dhahir, A. Zerguine, and A. Zidouri, "Adaptive frequency-domain RLS DFE for uplink MIMO SC-FDMA," *IEEE Trans. Veh. Technol.*, vol. 64, no. 7, pp. 2819–2833, Jul. 2015.
[31] S. Alamouti, "A simple transmit diversity technique for wireless communications," *IEEE J. Sel. Areas Commun.*, vol. 16, no. 8, pp. 1451–1458, Oct. 1998.
[32] Z. Yang, Y. Fang, G. Zhang, F. C. M. Lau, S. Mumtaz, and D. B. Da Costa, "Analysis and optimization of tail-biting spatially coupled protograph LDPC codes for BICM-ID systems," *IEEE Trans. Veh. Technol.*, vol. 69, no. 1, pp. 390–403, Jan. 2020.
[33] A. Chindapol and J. Ritcey, "Design, analysis, and performance evaluation for BICM-ID with square QAM constellations in Rayleigh fading channels," *IEEE J. Sel. Areas Commun.*, vol. 19, no. 5, pp. 944–957, May 2001.
[34] V. Lottici and M. Luise, "Embedding carrier phase recovery into iterative decoding of turbo-coded linear modulations," *IEEE Trans. Commun.*, vol. 52, no. 4, pp. 661–668, Apr. 2004.
[35] M. Marey, M. Samir, and O. A. Dobre, "EM-based joint channel estimation and IQ imbalances for OFDM systems," *IEEE Trans. Broadcast.*, vol. 58, no. 1, pp. 106–113, Mar. 2012.
[36] M. Marey, H. Mostafa, O. A. Dobre, and M. H. Ahmed, "Data detection algorithms for BICM alternate-relaying cooperative systems with multiple-antenna destination," *IEEE Trans. Veh. Technol.*, vol. 65, no. 5, pp. 3802–3807, May 2016.
[37] M. Marey and O. A. Dobre, "Iterative receiver design for uplink OFDMA cooperative systems," *IEEE Trans. Broadcast.*, vol. 62, no. 4, pp. 936–947, Dec. 2016.
[38] Y. A. Eldemerdash and O. A. Dobre, "On the identification of SM and Alamouti-coded SC-FDMA signals: A statistical-based approach," *IEEE Trans. Veh. Technol.*, vol. 65, no. 12, pp. 10079–10084, Dec. 2016.

MOHAMED MAREY (Senior Member, IEEE) received the M.Sc. degree in electrical engineering from Menoufia University, Egypt, in 1999, and the Ph.D. degree in electrical engineering from Ghent University, Belgium, in 2008. From 2009 to 2014, he was a Research Associate and a Visiting Professor with the Faculty of Engineering and Applied Science, Memorial University, Canada. He is currently a Full Professor with the Faculty of Electronic Engineering, Menoufia University. He is on a sabbatical leave in order to join Prince Sultan University, Saudi Arabia, as a Research Laboratory Leader of the Smart Systems Engineering Laboratory. He has authored the book *Multi-Carrier Receivers in the Presence of Interference: Overlay Systems* (VDM Publishing House Ltd., 2009) and around 100 scientific papers published in international journals and conferences. His main research interests include wireless communications and digital signal processing, with a particular focus on smart antennas, cooperative communications, signal classification for cognitive radio systems, synchronization and channel estimation, multiple-input multiple-output antenna systems, multi-carrier systems, and error correcting codes. He was a recipient of the Young Scientist Award from the International Union of Radio Science, in 1999. He is an Editor of IEEE Open Journal of the Communications Society.

HALA MOSTAFA (Member, IEEE) received the Ph.D. degree in electrical engineering from the Faculty of Engineering and Applied Science, Memorial University, Canada, in 2014. From 2014 to 2015, she was a Research Scientist at Memorial University. She is currently an Assistant Professor at the Information Technology Department, College of Computer and Information Sciences, Princess Nourah bint Abdulrahman University, Riyadh, Saudi Arabia. Her main research interests include wireless communications, with a particular focus on smart antennas and wireless sensor networks.